Polymer 50 (2009) 6218–6227

Contents lists available at ScienceDirect

Polymer

journal homepage: www.elsevier.com/locate/polymer

Enhanced fibroblast adhesion and proliferation on electrospun fibers obtained from poly(isosorbide succinate-*b*-L-lactide) block copolymers

Romeu Casarano [a], Ricardo Bentini [a], Vânia B. Bueno [a], Talita Iacovella [a,b], Fabiola B.F. Monteiro [b], Fábio A.S. Iha [a], Ana Campa [b], Denise F.S. Petri [a], Michael Jaffe [c], Luiz H. Catalani [a,*]

[a] Institute of Chemistry, University of São Paulo, São Paulo, Brazil
[b] Faculty of Pharmaceutical Sciences, University of São Paulo, São Paulo, Brazil
[c] Medical Device Concept Laboratory, New Jersey Institute of Technology, Newark, USA

ARTICLE INFO

Article history:
Received 7 August 2009
Received in revised form
19 October 2009
Accepted 19 October 2009
Available online 29 October 2009

Keywords:
Isosorbide
PLLA
Copolymer

ABSTRACT

Block copolymers containing isosorbide succinate and L-lactic acid repeating units with different mass compositions were synthesized in two steps: bulk ring-opening copolymerization from L-lactide and poli(isosorbide succinate) (PIS) preoligomer, in the presence of tin(II) 2-ethylhexanoate as catalyst, followed by chain extension in solution by using hexamethylene diisocyanate. Poly(L-lactide) (PLLA) and a chain extension product from PIS were also obtained, for comparison. SEC, ^{1}H and ^{13}C NMR, MALDI-TOFMS, WAXD, DSC, TG, and contact angle measurements were used in their characterization. The incorporation of isosorbide succinate into PLLA main backbone had minor effect on the thermal stability and the T_g of the products. However, it reduced the crystallinity and increased the surface energy in relation to PLLA. Nonwoven mats of the block copolymers and PLLA obtained by electrospinning technique were submitted to fibroblasts 3T3-L1 cell culture. The copolymers presented enhanced cell adhesion and proliferation rate as revealed by MTT assay and SEM images.

1. Introduction

Poly(acid lactic), PLA, is a generic name for the homopolymers containing acid lactic repeating units, while poly(L-lactide), PLLA, is generally used for polymers obtained from L-lactide, a cyclic diester of L-lactic acid, through ring-opening polymerization (ROP) [1,2]. PLA is a biodegradable and bioresorbable [3,4] aliphatic polyester well studied. On the other hand, a system relatively less studied but with increasing interest in the last decades is that composed of 1,4:3,6-dianhydrohexitols as diols and aliphatic or aromatic dicarboxylic acid derivatives [5–9], such as poly(isosorbide succinate) (PIS). Thiem and Lüders [10] have published one of the earliest application of isosorbide (1,4:3,6-dianhydro-D-glucitol), using terephthaloyl dichloride as aromatic dicarboxylic acid derivative, on a diol–diacid polyester synthesis. Direct incorporation of isosorbide into commercial polyesters such as poly(ethylene terephthalate), PET, can raise their glass transition temperatures [11] allowing a new range of applications including hot-fill containers [9]. In spite of the increasing interest in isosorbide use in aromatic (co)polyesters, relatively little is known about its effect on aliphatic copolyesters [8,12], especially on their surface properties and cell adhesion behavior.

The incorporation of glycolide or D,L-lactide moieties into PLLA main backbones produces copolymers with lower crystallinities, accelerating the (bio)degradation process [3], while the incorporation of ε-caprolactone or trimethylene carbonate gives rise to products with lower glass transition temperatures and crystallinities [13]. Besides, copolymers containing both glycolide and L-lactic acid mers are more hydrophilic than PLLA [13]. Although the hydrophilic character could be more advantageous for (bio)degradation rate than crystallinity reduction [3,14], it could not be favorable for scaffold materials used (i) in tissue engineering for cell adhesion, growing and proliferation, and (ii) in hydrolysable drug delivery systems. It was reported [15] that the incorporation of hydrophilic poly(ethylene glycol) and di(ethylene glycol) produced copolymers with higher hydrophilic character and lower cell adhesion than the homopolymer poly(3-hydroxybutyrate), PHB, an aliphatic polyester with hydrophobic character comparable to PLLA [16,17]. On the other hand, there has been some controversy in the literature on the role of hydrophobic vs hydrophilic character of the surface on cell adhesion [18,19].

Fibers are desirable as scaffold materials since they provide an appropriate substrate for migration and proliferation of cells. The

* Corresponding author. Instituto de Química, Universidade de São Paulo, CP 26077, 05513-970, São Paulo, Brasil. Tel.: +55 11 3091 3162; fax: +55 11 3815 5579.
E-mail address: catalani@usp.br (L.H. Catalani).

0032-3861/$ – see front matter © 2009 Elsevier Ltd. All rights reserved.
doi:10.1016/j.polymer.2009.10.048

traditional techniques used for fiber productions, such as wet spinning, dry spinning and melt spinning, allow obtaining fibers with average diameters ranging from 10 to 500 μm [20]. On the other hand, electrostatic spinning or electrospinning is an interesting technique to attain fibers with much smaller diameters, varying from 10 nm to 10 μm [21,22]. Electrospinning studies typically involve polymers with high average molar masses, since chain entanglements are required for the formation of electrospun fibers [23,24]. Nonwoven mats can be obtained by electrospinning from polymer solution or melt. Poly(α-hydroxy acids) are the polymer class most known and largely employed in the production of nanofibers for medical applications [25].

The objective of this work is to synthesize aliphatic block copolyesters containing isosorbide succinate (IS) and L-lactic acid (LLA) repeating units with average molar masses high enough to allow electrospun fibers to be produced. The use of the electrospun mats as scaffolds for cell culture was investigated in order to evaluate the influence of isosorbide succinate mers on adhesion, growth and proliferation of fibroblast 3T3-L1 cells.

2. Experimental

2.1. Materials

Succinic anhydride (Aldrich; 97%) was refluxed with acetic anhydride for 30 min, filtered, and washed with dry ethyl ether (m.p. = 120.8–120.9 °C). L-lactide (99.5%; m.p. = 98.7–98.8 °C) was kindly supplied by Purac and used without further purification. Isosorbide (Aldrich; 98%) was recrystallized (m.p. = 63.5–63.6 °C) from dry ethyl acetate. Hexamethylene diisocyanate (HDI; Aldrich; 98%), tin(II) 2-ethylhexanoate ($SnOct_2$; Aldrich; ~95%), analytical grade anhydrous methanol (Carbo Erba) and analytical grade chloroform (Vetec) were used as received.

2.2. Characterization

Size exclusion chromatography (SEC) measurements of $\overline{M}_n$ and $\overline{M}_w$ were performed in a Shimadzu HPLC class-VP system equipped with a Shimadzu RID 10A differential refractive index detector and connected to four Styragel columns (10^2, 10^3, 10^4, and 10^5 Å; Waters). Chloroform was used as mobile phase (1 mL min^{-1}) and polystyrene (PS) reference samples (Aldrich/Waters) were used for calibration.

^{1}H and ^{13}C nuclear magnetic resonance (NMR) spectroscopy experiments were carried out in a Bruker AC 200E (200 and 50 MHz), except for 2-D NMR measurements (Bruker DRX 500–500 and 125 MHz). The chemical shifts (δ) were referenced to TMS and the measurements were performed by using $CDCl_3$ solutions.

Matrix-assisted laser desorption/ionization time-of-flight mass spectrometry (MALDI-TOFMS) measurements were performed in an Ettan MALDI-TOF mass spectrometer (Amersham Biosciences), previously calibrated [8], using an acceleration voltage of 20 kV and nitrogen laser (337 nm). 200 laser shots were added and the positive ions detection was carried out in reflection mode. The solutions were prepared in chloroform/tetrahydrofuran (THF) (1:1, v/v) while 1,8,9-trihydroxyanthracene (dithranol) and NaI were used as matrix and cationizing agent, respectively.

Differential scanning calorimetry (DSC) measurements were performed in a Mettler-Toledo DSC-822 calorimeter previously calibrated with In and Zn as references. Typically, samples weighting about 7 mg were heated (10 °C min^{-1}) in Al crucibles from −20 to 200 °C, cooled (10 °C min^{-1}) to −20 °C, and heated again (10 °C min^{-1}) to 200 °C, under N_2 atmosphere (100 mL min^{-1}). The second run was considered for determining the glass transition (T_g), crystallization (T_c), and melting (T_m) temperatures, as well as the heat of fusion (ΔH_m). The degree of crystallinity ($W_{c,h}$) was calculated by dividing ΔH_m by the heat of fusion for a PLLA sample extrapolated to 100% crystalline as 93 J g^{-1} [26] and then multiplying the aftermath by 100.

Thermogravimetry (TG) analyses were carried out with a TA Instruments, Hi-Res™ TGA 2950. The samples (8–12 mg) were heated from 35 to 600 °C at a heating rate of 10 °C min^{-1}, using Pt crucible and N_2 atmosphere (100 mL min^{-1}).

The diffraction patterns of wide angle X-ray diffraction (WAXD) were performed in a Rigaku Miniflex powder X-ray diffractometer, using a monochromatic beam with wavelength (λ) of 0.154 nm (CuK_α), voltage of 30 kV, and electric current of 15 mA. The intensities were collected from 2θ values ranging from 3 to 60° with steps of 0.02°. Prior to the analyses, the powdered samples were annealed in a vacuum-oven at 90 °C for 48 h, while the solution-cast films (thicknesses of 50–60 μm) were annealed in consecutive steps (in order to avoid bubble formation) at 40 °C for 24 h, 50 °C for 24 h, 60 °C for 24 h, 70 °C for 24 h, and 80 °C for 48 h, unless otherwise stated. The degree of crystallinity ($W_{c,x}$) of the annealed samples was obtained from the corresponding diffraction profiles with curve decompositions following Gaussian function adjusts by dividing the area of crystalline peaks by the total area (crystalline peaks plus amorphous halo) and then multiplying the result by 100.

Surface energy was determined indirectly by contact angle measurements in a home-built apparatus [27], using the sessile drop method. Thin films (thicknesses of ~60–100 nm, obtained by ellipsometry in a Ratzeburg DRE-EL02 using an incidence angle of 70° and He–Ne laser of $\lambda = 632.8$ nm) were prepared by spin coating (in a Headway PWM32-OS-RT90 spin coater) the polymeric solutions (at 10 mg mL^{-1}) in chloroform onto Si/SiO_2 wafers. The solutions were previously filtered by means of 0.45 μm filters (MilliPore). Distilled water (or diiodomethane; Aldrich) sessile drops of 8 μL were used for contact angle measurements (θ). The data represent averages with the corresponding standard deviations calculated from three replicates.

Scanning electron microscopy (SEM) was performed in a Jeol JSM 7401 F from samples with or without Au-protective coating.

2.3. Synthesis and purification

PLLA was obtained in bulk by ROP as follows: L-lactide (10.1 g; 7.0×10^{-2} mol) and $SnOct_2$ (19 mg; 4.7×10^{-5} mol) were added to an ampoule under argon atmosphere, then the ampoule was sealed under vacuum at ~1 mmHg and placed into an oil bath maintained at 120–130 °C for 165 h. A small aliquot of $SnOct_2$ solution in dry chloroform was taken. PIS was synthesized in bulk by step polymerization as follows: isosorbide (11.9 g; 8.1×10^{-2} mol), succinic anhydride (8.13 g; 8.1×10^{-2} mol), and $SnOct_2$ (1.00 g; 2.5×10^{-3} mol) were added to a one-neck round-bottom flask under argon atmosphere. The closed flask was placed into an oil bath, kept at 140–160 °C for 7 h, then vacuum was applied and the reaction continued for additional 2 h at 30–40 mmHg and 22 h at ~1 mmHg. The reaction conditions were based on modified literature data [7].

Each sample of the product **1** was synthesized in bulk from ring-opening copolymerization as follows: L-lactide, PIS, and $SnOct_2$ (via small aliquots from solutions in dry chloroform) were added to an ampoule under argon atmosphere. The ampoule was then sealed under vacuum at ~1 mmHg and placed into an oil bath kept at 120–130 °C for 165 h. Every sample of the product **2** (or **3**) was obtained in solution from chain extension as follows: **1** (or PIS), HDI, and dry chloroform were added to one-neck round-bottom flask under argon atmosphere. Then, the reaction was allowed to proceed in reflux under N_2 atmosphere for 24 h in an oil bath kept at 63–73 °C and in RT for an additional week. In the case of **3**, the

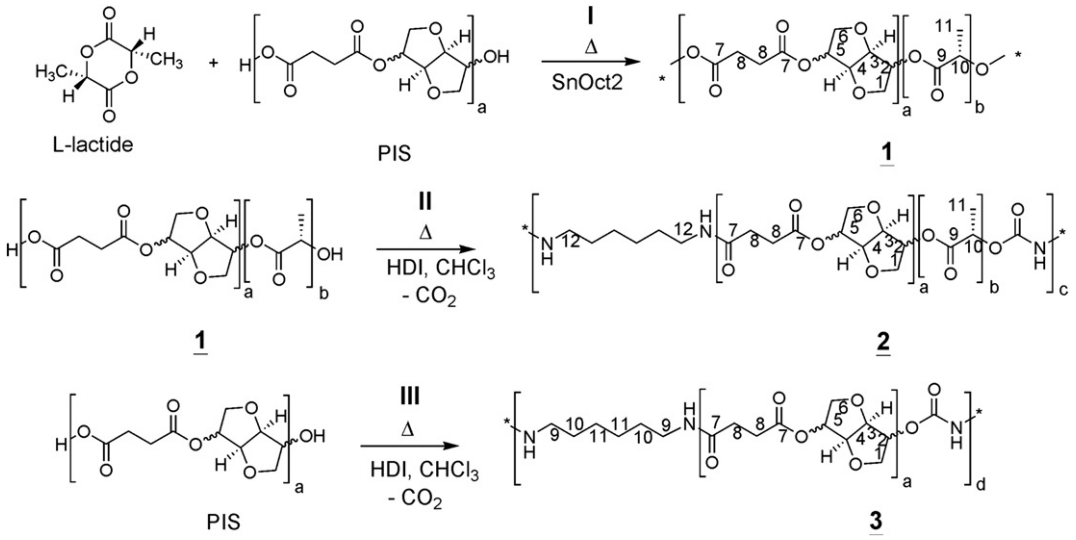

Scheme 1. Proposed chemical structures for poly(isosorbide succinate-*b*-L-lactide), **1**, and for the chain extension products **2** and **3** obtained from **1** and PIS, respectively.

reaction was continued: it was added more HDI (half of the predefined quantity) and chloroform, then the reaction proceeded in a similar manner as previously described. The quantities used to attain **1**–**3** (see Scheme 1) are given in Table 1.

The purification was performed by means of a solvent (chloroform; 1v) and a non-solvent (methanol; 10v) then the filtrated was dried in a vacuum-oven at 45 °C for 48 h. The yields obtained for PLLA and PIS were 85% and 90%, while the values of $\overline{M}_n$ and $\overline{M}_w$ were 96,000 and 180,000 g mol^{-1} and 2,700 and 5,600 g mol^{-1}, respectively. Those obtained for **1**–**3** are displayed in Table 1, as well as the respective mass compositions.

1: ^{1}H NMR (200 MHz, in $CDCl_3$): δ (in ppm): 5.21–5.11 (3H; H-2, H-5, H-10); 4.82 (1H; H-4); 4.47 (1H; H-3); 3.96 (2H; H1a,b); 3.91 (1H; H-6a or b); 3.81 (1H; H-6b or a); 2.70 (4H; H-8); 1.58 (3H; H-11). ^{13}C NMR (50 MHz, in $CDCl_3$): δ (in ppm): 171.4 and 171.1 (2C; C-7); 169.4 (C-9); 85.6 (C-3); 80.6 (C-4); 78.1 (C-2); 74.1 (C-5); 73.0 (C-1); 70.2 (C-6); 68.8 (C-10); 28.7 and 28.5 (2C; C-8); 16.5 (C-11).

2: ^{1}H NMR (200 MHz, in $CDCl_3$): δ (in ppm): 5.21–5.11 (3H; H-2, H-5, H-10); 4.82 (1H; H-4); 4.47 (1H; H-3); 3.96 (2H; H1a,b); 3.91 (1H; H-6a or b); 3.81 (1H; H-6b or a); 3.16* (4H; H-12); 2.68 (4H; H-8); 1.58 (3H; H-11). * It appears at a resonance of very low intensity. ^{13}C NMR (50 MHz, in $CDCl_3$): δ (in ppm): 171.5 and 171.2 (2C; C-7); 169.6 (C-9); 85.8 (C-3); 80.7 (C-4); 78.2 (C-2); 74.3 (C-5); 73.2 (C-1); 70.4 (C-6); 69.0 (C-10); 28.8 and 28.6 (2C; C-8); 16.6 (C-11).

3: ^{1}H NMR (200 MHz, in $CDCl_3$): δ (in ppm): 5.20–5.15 (2H; H-2, H-5); 4.82 (1H; H-4); 4.47 (1H; H-3); 3.96 (2H; H1a,b); 3.91 (1H; H-

Table 1
Syntheses parameters of **1**–**3**.

Product	Reagent 1	Reagent 2	Solvent	Catalyst	Yield (%)	$\overline{M}_n$ (g mol^{-1})[a]	$\overline{M}_w$ (g mol^{-1})[a]
1$_{86\text{-}14}$[b]	L-lactide 8.50 g; 5.9×10^{-2} mol	PIS 1.50 g; $\overline{M}_n = 2{,}700$ g mol^{-1}	–	$SnOct_2$ 16 mg; 3.9×10^{-5} mol	82	28,000	54,000
1$_{74\text{-}26}$[b]	L-lactide 7.00 g; 4.9×10^{-2} mol	PIS 3.00 g; $\overline{M}_n = 2{,}700$ g mol^{-1}	–	$SnOct_2$ 13 mg; 3.2×10^{-5} mol	88	12,000	28,000
1$_{64\text{-}36}$[b]	L-lactide 6.00 g; 4.2×10^{-2} mol	PIS 4.00 g; $\overline{M}_n = 2{,}700$ g mol^{-1}	–	$SnOct_2$ 11 mg; 2.7×10^{-5} mol	83	8,200	21,000
2$_{86\text{-}14}$[b]	**1**$_{86\text{-}14}$ 4.00 g; $\overline{M}_n = 28{,}000$ g mol^{-1}	HDI[c] 42 mg; 2.5×10^{-4} mol	$CHCl_3$ 25 mL –	–	85	67,000	130,000
2$_{74\text{-}26}$[b]	**1**$_{74\text{-}26}$ 4.00 g; $\overline{M}_n = 12{,}000$ g mol^{-1}	HDI[c] 83 mg; 4.9×10^{-4} mol	$CHCl_3$ 25 mL –	–	86	57,000	130,000
2$_{64\text{-}36}$[b]	**1**$_{64\text{-}36}$ 4.00 g; $\overline{M}_n = 8{,}200$ g mol^{-1}	HDI[c] 107 mg; 6.4×10^{-4} mol	$CHCl_3$ 25 mL –	–	85	50,000	130,000
3	PIS[d] 7.00 g; $\overline{M}_n = 2{,}700$ g mol^{-1}	HDI[c,d] 810 mg; 4.8×10^{-3} mol	$CHCl_3$[d] 80 mL –	–	57[e]	26,000	57,000

[a] Determined by SEC.
[b] The subscripts refer to the mass composition of L-lactic acid and isosorbide succinate repeating units obtained by ^{1}H NMR, respectively.
[c] HDI:**1** or PIS molar ratios: 1.7:1.0, 1.5:1.0, 1.3:1.0, and 1.9:1.0, respectively.
[d] The total amount was added in two steps.
[e] It was formed a certain amount of insoluble gel that was removed by filtration prior to purification step.

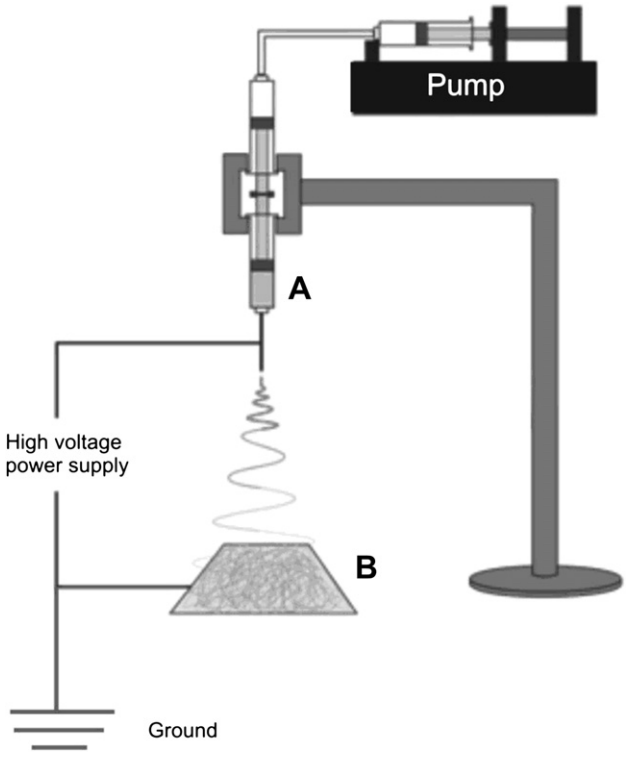

Fig. 1. Schematic representation of the apparatus used to obtain nonwoven mats by electrospinning from (co)polymer solutions. *A* is the syringe plus the needle and *B* is the collector, a plate of stainless steel.

6a or b); 3.83 (1H; H-6b or a); 3.16* (4H; H-9); 2.67 (4H; H-8); 1.49* (4H; H-10); 1.33* (4H; H-11). * They appear at resonances of very low intensities. ^{13}C NMR (50 MHz, in $CDCl_3$): δ (in ppm): 171.3 and 171.0 (2C; C-7); 85.6 (C-3); 80.5 (C-4); 78.0 (C-2); 74.1 (C-5); 73.0 (C-1); 70.2 (C-6); 28.7 and 28.5 (2C; C-8).

2.4. Electrospinnig

Fig. 1 illustrates the schematic representation of the apparatus employed to obtain nonwoven mats by electrospinning from the respective (co)polymer solutions. Conditions: needle diameter 0.584 mm, effective syringe volume 6 mL, solvent 65% dichloromethane and 35% *N*,*N*-dimetilformamide (v/v), voltage 24 kV, feed rate 3 mL h^{-1}, and working distance 24 cm.

2.5. Cell adhesion and proliferation

The cells used were fibroblasts 3T3-L1 (Swiss albino mouse) from Rio de Janeiro Cell Bank, Federal University of Rio de Janeiro, Brazil. Round samples of the nonwoven mats of ~5 mm diameter were previously dried in a vacuum-oven at 40 °C for three days. The nonwoven mats were laid into 96-well cell culture plates and irradiated for 30 min with UV light. 200 μL of Dulbecco's modified Eagle's medium (DMEM) supplemented with 10% of calf serum and 1% of penicillin/streptomycin (10,000 U mL^{-1}/10,000 μg mL^{-1}) were added. After two days in an oven at 37 °C under a 5% CO_2 atmosphere, the culture medium was removed. A cell suspension in DMEM was prepared (from previously trypsinized cells) at a concentration of 25,000 cell mL^{-1} and aliquots of 100 μL were added to each well. After the elapsed time of 24, 48, 72, 96, 120, and 240 h the supernatant was removed. For SEM measurements the cultured spun mats were washed twice with PBS, the cells fixed with formalin at 10 wt% and dehydrated by changing the medium with an aqueous solution with increasing concentration of ethanol (25, 50, 70, 90, 95 and 100%) for 10 min each, and finally lyophilized.

2.6. MTT assay

The cultured spun mats were washed twice with PBS and placed in a new well plate and 160 μL of DMEM (without calf serum) plus 40 μL of 5 mg mL^{-1} aqueous solution of 3-(4,5-dimethylthiazol-2-yl)-diphenyltetrazoliumbromide (MTT; a tetrazole) were added into every well. After 3 h in the oven, the solution was removed, 200 μL of dimethyl sulfoxide was added to each well and the plate was stirred for 20 min. Aliquots of 200 μL were taken and poured into new 96-well cell culture plates in order to measure the absorbance at 490 nm (SLT-Spectra, Salzburg, Austria). The data reported are averages calculated from three samples of each condition. The significance of the results was analyzed by two-way ANOVA test.

3. Results and discussion

3.1. Synthesis of IS-LLA chain extended block copolymers

In our previous work [8] four low molecular weight copolymers containing L-lactic acid, isosorbide, and succinate moieties were synthesized in bulk from four distinct synthetic approaches, namely: (i) from L-lactide, isosorbide, succinic anhydride, and $SnOct_2$; (ii) from PLLA, isosorbide, and succinic anhydride; (iii) from PIS, L-lactide, and $SnOct_2$; and (iv) from PLLA, PIS, and $SnOct_2$. The first approach allowed the production of a random copolymer and the last three gave rise to block copolymers. The synthetic approach (iii), starting from PIS, L-lactide, and $SnOct_2$, was chosen to test the viability of the obtained copolymer as scaffold material for fibroblast culture.

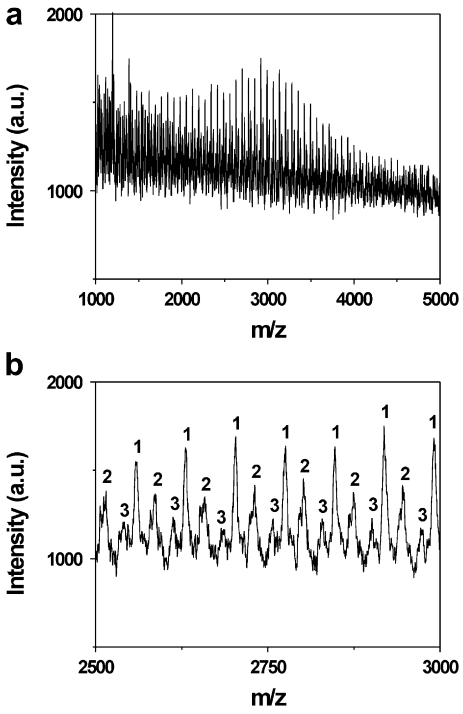

Fig. 2. MALDI-TOF mass spectra obtained for $\underline{1}_{74\text{-}26}$ in (a) full region and (b) expanded region at *m*/*z* ranging from 2500 to 3000.

Table 2
WAXD and DSC results for 1-3.

Run	WAXD	DSC[g]				
	$W_{c,x}$[a]	T_g	T_c	T_m	ΔH_m	$W_{c,h}$[b]
	(%)	(°C)	(°C)	(°C)	(J g^{-1})	(%)
PLLA	64[c]	57	n.o.[e]	175	54	58 (50)[f]
PIS	—	56	n.o.[e]	n.o.[e]	—	—
1$_{86\text{-}14}$	59[d]	57	100	162	50	54 (56)[f]
1$_{74\text{-}26}$	53[d]	54	113	155	25	27 (31)[f]
1$_{64\text{-}36}$	38[d]	58	121	156	32	34 (40)[f]
2$_{86\text{-}14}$	49[c]	61	n.o.[e]	164	34	37 (45)[f]
2$_{74\text{-}26}$	38[c]	58	n.o.[e]	155	23	25 (12)[f]
2$_{64\text{-}36}$	26[c]	63	n.o.[e]	155	1	1 (27)[f]
3	—	62	n.o.[e]	n.o.[e]	—	—

[a] Degree of crystallinity obtained by WAXD.
[b] Degree of crystallinity from the second run calculated using heat of fusion of 93 J g^{-1} for PLLA sample extrapolated to 100% crystallinity [26].
[c] From solution-cast films (previously annealed at 40 °C for 24 h, 50 °C for 24 h, 60 °C for 24 h, 70 °C for 24 h, and 80 °C for 48 h).
[d] From powdered samples (earlier annealed at 90 °C for 48 h).
[e] Not observed.
[f] Calculated from heat of fusion acquired during the first heating, for comparison.
[g] From as-purified samples.

Product **1** (Scheme 1) was synthesized in bulk via ring-opening copolymerization of L-lactide and PIS preoligomer, in the presence of $SnOct_2$ as catalyst with three different mass compositions in terms of LLA and IS: 86 and 14%, 74 and 26%, and 64 and 36%, coded as **1**$_{86\text{-}14}$, **1**$_{74\text{-}26}$, and **1**$_{64\text{-}36}$, respectively. The mass compositions obtained are closely related to the composition on the feed. As it can be seen in Table 1, as PIS composition in the feed increases, the average molar mass decreases, giving evidence that PIS hydroxyl end groups act as reaction initiators of the ring-opening polymerization reactions [28,29]. The reaction yields ranged from 82 to 88%, while $\overline{M}_w$ values varied from 21,000 to 54,000 g mol^{-1}.

Chain extended product **2** was obtained in solution from the reaction of **1** with hexamethylene diisocyanate as chain extensor. The products presented LLA to IS mass composition ratios identical to its reagent and were identified as **2**$_{86\text{-}14}$, **2**$_{74\text{-}26}$, and **2**$_{64\text{-}36}$ (Table 1). The reaction yields varied from 85 to 86% and $\overline{M}_w$ values raised 2–6 times regarding those of the starting materials. By reacting PIS with the chain extensor, in solution, product **3** was obtained with $\overline{M}_w$ 10 times greater than that of PIS (*cf.* experimental part and Table 1). In this case the reaction yield was relatively low due to the partial formation of insoluble gel, which was properly removed before the final purification. The isocyanate functional groupings of HDI molecules are capable of reacting not only with hydroxyl and carboxyl groups, yielding, respectively, urethanes and amides (from the loss of CO_2 of the thermally unstable *N*-carboxyanhydrides), but also with other functional groups like amine, urea, urethane, and amide [30]. The reaction of isocyanates with urethane and amide groups produces allophanates and acyl ureas. Therefore, HDI, whose molecules contain two isocyanates, could lead to the formation of cross-links, resulting in gel formation. Kylmä e Seppälä [31] have reported the formation of gel of up to 75 wt% from chain extension of copolymers, produced from L-lactic acid, ε-caprolactone, and 1,4-butanediol, using an aromatic diisocyanate.

Table 3
WAXD results for the solution-cast films obtained from **2** after additional annealing of 3, 6 and 9 days at 80 °C.

Run	$W_{c,x}$ (%)[a]		
	After 3 days	After 6 days	After 9 days
2$_{86\text{-}14}$	48	52	–
2$_{74\text{-}26}$	47	51	–
2$_{64\text{-}36}$	–	38	40

[a] Degree of crystallinity obtained by WAXD.

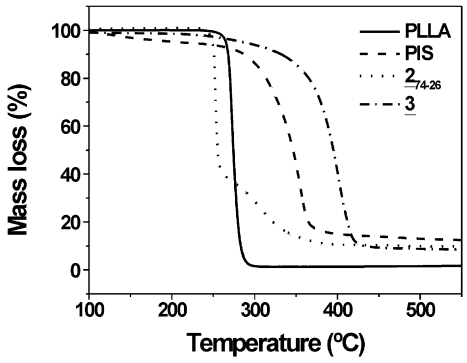

Fig. 3. Typical TG curves acquired for PLLA, PIS, **2**$_{74\text{-}26}$, and **3**.

3.2. Structural characterization of the chain extended copolymers

^{1}H and ^{13}C typical peak assignments from isosorbide moieties presented in **1**–**3** were based on 2-D NMR (^{1}H–^{1}H COSY, ^{1}H–^{13}C HSQC, and ^{1}H–^{13}C HMBC) carried out for **1**$_{74\text{-}26}$ (Supplementary Material 1). ^{13}C NMR spectra obtained for the samples of **1** and **2** in the carbonyl region did not display additional peaks (Supplementary Material 2), consistent with bock copolymer structures [8,32].

Copolymer structures of the samples of **1** were evidenced by MALDI-TOFMS by observing a good agreement between experimental and calculated *m*/*z* data. Typical MALDI-TOF mass spectra obtained for one of the samples of **1** at *m*/*z* range of 2500–3000, arbitrarily chosen, are illustrated in Fig. 2. The peak series displayed in Fig. 2(b) and identified as 1 were ascribed by considering the proposed chemical structure for adducts of **1**$_{74\text{-}26}$ as being $[Na\text{-}(IS)_a\text{-}(LLA)_b\text{-}OH + Na^+]^{+1}$ and using the equation $m/z = 228a + 72b + 40 + 23$, where *a* and *b* are isosorbide succinate and L-lactic acid repeating units, 228 and 72 refer to the relative molar masses of isosorbide succinate and L-lactic acid repeating units, 40 corresponds to the relative atomic mass of sodium atom plus the relative molar mass of hydroxyl end group [8,33], and 23 stands for the relative atomic mass of Na^+. The calculated *m*/*z* values (*a*,*b*) for the peak series 1 are 2559 (4,22), 2631 (4,23), 2703 (4,24), 2775 (4,25), 2847 (4,26), 2919 (4,27), and 2991 (4,28), in good agreement with the experimental data 2558.2, 2630.3, 2703.4, 2775.7, 2847.3, 2918.9, and 2991.3. In a similar manner, the peak series marked as 2 and 3 were assigned by taking into account the proposed chemical

Table 4
Advancing contact angle measurements and surface energy data.[a]

Run	θ_a (°)[b]		Surface energy (mN m^{-1})[c]		
	(H_2O)	(CH_2I_2)	γ_s	γ_s^d	γ_s^p
PLLA	82 ± 2	54 ± 2	40 ± 2	33 ± 2	7 ± 2
2$_{86\text{-}14}$	72 ± 2	35 ± 1	53 ± 2	42 ± 2	11 ± 2
2$_{74\text{-}26}$	82 ± 2	22 ± 1	54 ± 2	47 ± 2	7 ± 2
2$_{64\text{-}36}$	82 ± 2	23 ± 2	54 ± 2	47 ± 2	7 ± 2
3	66 ± 3	18 ± 1	62 ± 3	48 ± 3	14 ± 3
Collagen[d]	–	–	48[d]	–	–

[a] Using Si/SiO_2 wafers as substrates. The data are expressed in terms of average and standard deviation.
[b] Advancing contact angle measurements in water or in diiodomethane sessile drops.
[c] The surface energy was calculated [44,45] by using the advancing contact angle measurements in water and diidomethane sessile drops and Wu's harmonic mean method, besides the decomposition of the surface energy (γ_s) into the dispersive component (γ_s^d) and polar one (γ_s^p).
[d] From literature [49].

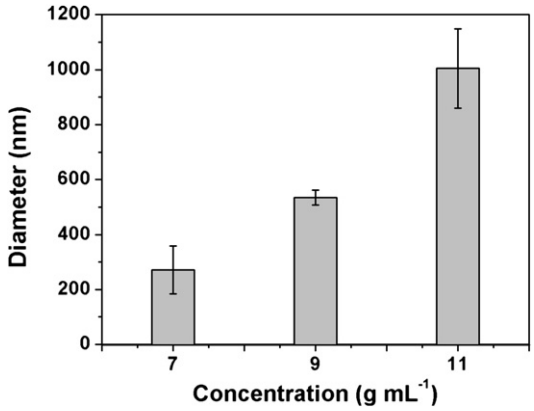

Fig. 4. Variation of the average diameter of the fibers in function of the concentration obtained for $\underline{\mathbf{2}}_{\mathbf{74\text{-}26}}$ by electrospinning.

structure for adducts of $\underline{\mathbf{1}}_{\mathbf{74\text{-}26}}$ as being $[\text{H-(IS)}_a\text{-(LLA)}_b\text{-OH} + \text{H}^+]^{+1}$ and applying the equation $m/z = 228a + 72b + 18 + 1$, where 18 refers to the relative molar masses of hydrogen atom and hydroxyl end group, and 1 corresponds to the relative atomic mass of H^+. The calculated m/z values (a,b) for the peak series 2 are 2515 (4,22), 2587 (4,23), 2659 (4,24), 2731 (4,25), 2803 (4,26), 2875 (4,27), and 2947 (4,28), against experimental data attained as 2515.3, 2585.9, 2658.5, 2731.1, 2801.8, 2874.7, and 2945.6. Similarly the peak series 3 amount to 2539 (6,16), 2611 (6,17), 2683 (6,18), 2755 (6,19), 2827 (6,20), 2899 (6,21), and 2971 (6,22), whereas the experimental data obtained were 2539.9, 2612.3, 2682.4, 2757.5, 2826.7, 2901.2, and 2971.9. In both cases, the experimental and calculated m/z data exhibited a good agreement. The appearance of odd and even numbers of L-lactic acid mers is an indication that side trans-esterification reactions took place during the synthesis of **1**. Data from literature [5,23–25] show odd and even numbers of L-lactic acid repeating units obtained by MALDI-TOFMS for both PLLA almost 100% isotactic and block copolymers containing PLLA sequences.

3.3. Crystallinity and thermal properties of the chain extended copolymers

The diffraction profile obtained by WAXD for **3** (Supplementary Material 3) is similar to that of PIS [8], showing only an amorphous halo, characteristic of non-crystalline samples. On the other hand, the diffraction patterns obtained by WAXD for powdered previously annealed samples from **1** and for solution-cast films from **2** and PLLA, also previously annealed, are typical of semicrystalline products (Supplementary Material 3). Because of the fibrous aspect of the samples of **2**, **3** and PLLA, the assays were performed with films. The degrees of crystallinity (Table 2) were attained from the diffraction profile decompositions following Gaussian function fits. As expected [8], the degrees of crystallinity are reduced with the increase of IS incorporation into PLLA main backbone. The corresponding ratios observed between the degrees of crystallinity obtained from solution-cast films (**2**) and from powdered samples (**1**) were 0.83, 0.72, and 0.68. The degrees of crystallinity attained from powdered samples are greater than those from films. Although they were obtained from different samples, the findings could suggest that (i) the crystallization rate of the powdered samples appeared to be higher than that of the films and (ii) PIS blocks seemed to inhibit even more the crystallization of solution-cast films. Bluhm et al. [34] have reported that films obtained from solution or melt, especially for copolymers composed of 3-hydroxybutyrate and 3-hydroxyvalerate, tend to crystallize much slower than the respective powdered samples and might demand several weeks (of annealing) to reach the equilibrium crystallinity. Furthermore, they also stated that if degrees of crystallinity were determined by WAXD before the equilibrium crystallinity was attained the data appeared to be composition dependent, as it seems to be with our findings.

In order to check whether or not the equilibrium crystallinity has been reached for the solution-cast films, the samples (previously annealed in consecutive steps at 40 °C for 24 h, 50 °C for 24 h, 60 °C for 24 h, 70 °C for 24 h, and 80 °C for 48 h) were additionally annealed for 3, 6 and 9 days. The respective diffraction profiles obtained by WAXD are displayed in Supplementary Material 4, whereas the corresponding degrees of crystallinity are shown in Table 3. These findings suggest that at least 6 additional days may be necessary for crystallinity to reach equilibrium (*cf.* Tables 2 and 3).

The glass transition temperature, crystallization temperature, melting temperature, heat of fusion, and degree of crystallinity determined by DSC are also summarized in Table 2. The T_g values obtained for both PIS and **1**–**3** are comparable to that of PLLA, in general. The presence of PIS blocks in **1** and **2** gave rise to a reduction of 13–20 °C in T_m, in relation to that of PLLA. The degrees of crystallinity obtained by DSC from the second heating for the samples of **1** and **2** are lower than that of PLLA, as observed earlier with WAXD results. Furthermore, the values obtained by DSC for **1** and **2**, as well as for PLLA, are comparatively lower than those of WAXD. Shyamroy et al. [35] also observed higher degrees of crystallinitiy obtained by WAXD (67–85%) than by DSC (39–51%) for PLLA. According to Wang et al. [36] degrees of crystallinity obtained by WAXD for semicrystalline samples are preferable since semicrystalline samples tend to undergo recrystallization during DSC measurements. Another problem concerning DSC measurements is that associated with the conflicting literature data for heat of fusion of PLLA 100% crystalline, which range from 83 to 148 J g^{-1} [36]. The degree of crystallinity obtained for $\underline{\mathbf{2}}_{\mathbf{64\text{-}36}}$ by DSC is very low (Table 2), which could be due to the slower crystallization rate of the sample from the melt. Some polyester samples based on isomannide (1,4:3,6-dianhydro-D-mannitol) or isoidide (1,4:3,6-dianhydro-L-iditol) and terephthalic acid synthesized by Storbeck et al. [37] showed endothermic melting transitions only during the first heating, while WAXD data revealed that those samples exhibited semicrystallinity. The authors stated that the products only crystallize from solution (during the purification step) [37].

Fig. 3 displays typical TG curves obtained for PLLA, PIS, **2**, and **3**. Thermogravimetric analysis shows that PLLA, PIS, and **3** displayed

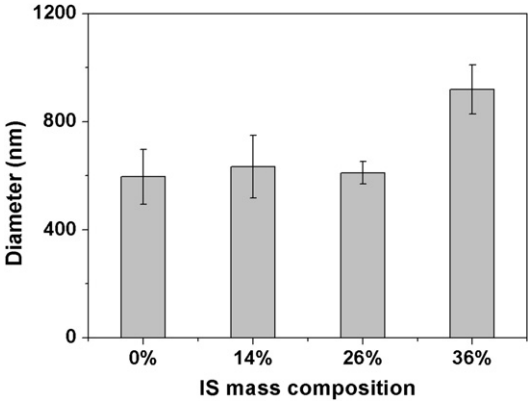

Fig. 5. Variation of the average diameter of the fibers in function of the mass composition of isosorbide succinate mers obtained for the samples of **2** by electrospinning. Concentration: 9% (w/v), except for PLLA, 5% (w/v), used for comparison.

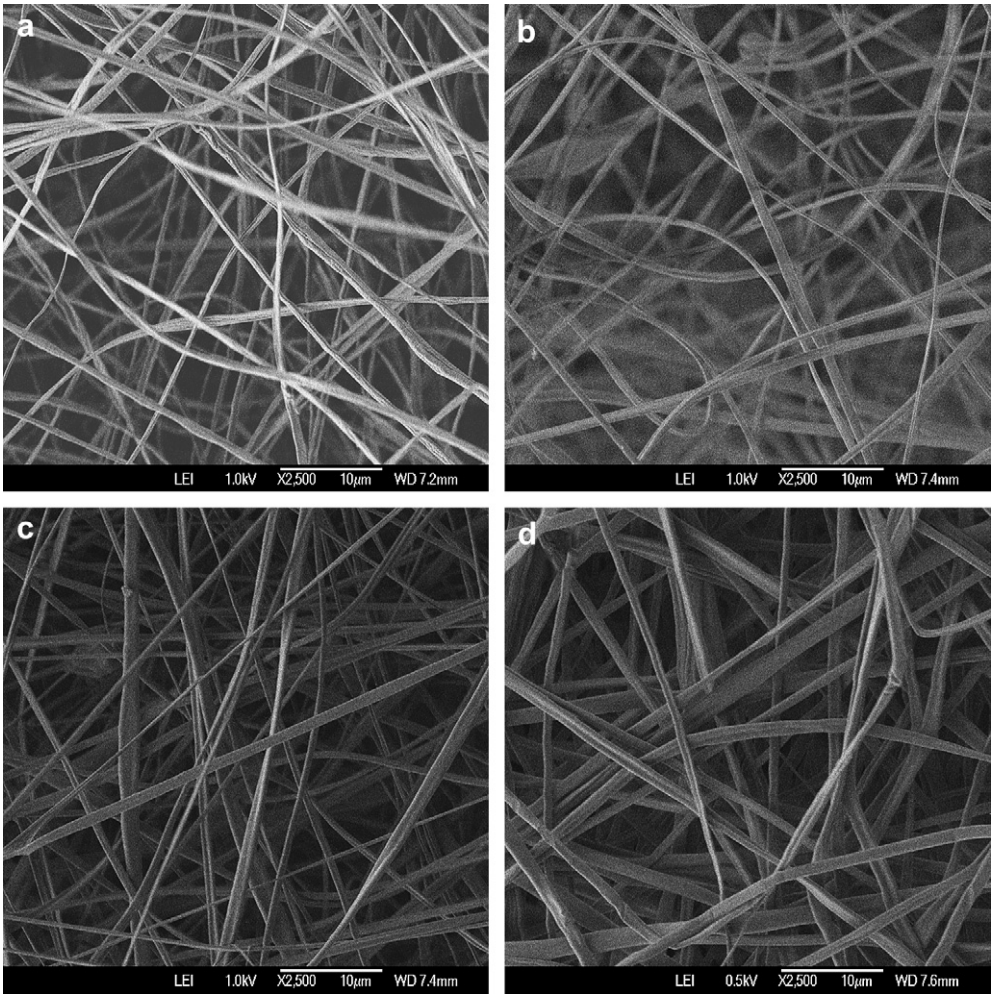

Fig. 6. SEM images of the nonwoven mats obtained by electrospinning for (a) PLLA, (b) **2**$_{86\text{-}14}$, (c) **2**$_{74\text{-}26}$, and (d) **2**$_{64\text{-}36}$. Concentration: 9% (w/v), except for PLLA, 5% (w/v), used for comparison. Magnification: 2500×. Scale bar: 10 μm.

one-step thermal decomposition. PIS and **3** showed very distinct TG curves as compared with that of PLLA. Although they presented similar thermal stability, the final decomposition temperatures observed for PIS and **3** are higher than that of PLLA. These results are explained by the presence of isosorbide moieties where primary decomposition leads to ring-opening without mass loss. PIS and **3** have similar TG curves, showing no effect of the chain extension. **2** showed two-step thermal decomposition and presented mass loss amount in each step approximately proportional to the mass composition of PLLA and PIS blocks. The presence of IS did not improve its thermal stability, as it was expected based on the good thermal stability of isosorbide monomer [38,39].

3.4. Contact angle measurements

The characteristic wettability of a material is given by advancing contact angle measurements [40]. A surface is considered hydrophobic when the advancing contact angle in water is >65° [41]. It is known that PLLA is relatively hydrophobic [42,43]. Table 4 gives the advancing contact angle (θ_a) measurements using Si/SiO_2 wafers as substrates and water as testing solvent. The advancing contact angle obtained for PLLA is in very good agreement with the data reported by Janorkar et al. (82°) [42] and is higher than that of **3**, meaning that PLLA is more hydrophobic than **3** (resulting from PIS chain extension). The presence of IS caused change only in **2**$_{86\text{-}14}$ (Table 4). Fowkes has suggested that the surface energy should be considered as a sum of independent contributions, each representing a particular intermolecular force [40]. From a practical

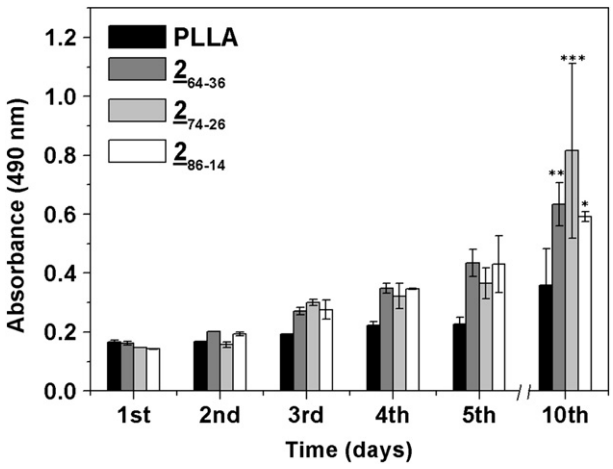

Fig. 7. MTT assay obtained from the nonwoven mats using 3T3-L1 cells. Two-way ANOVA test carried out for **2** for the period of 10 days: *Significant difference ($p < 0.05$) for **2**$_{86\text{-}14}$; **significant difference ($p < 0.01$) for **2**$_{64\text{-}36}$; ***significant difference ($p < 0.001$) for **2**$_{74\text{-}26}$, in relation to PLLA.

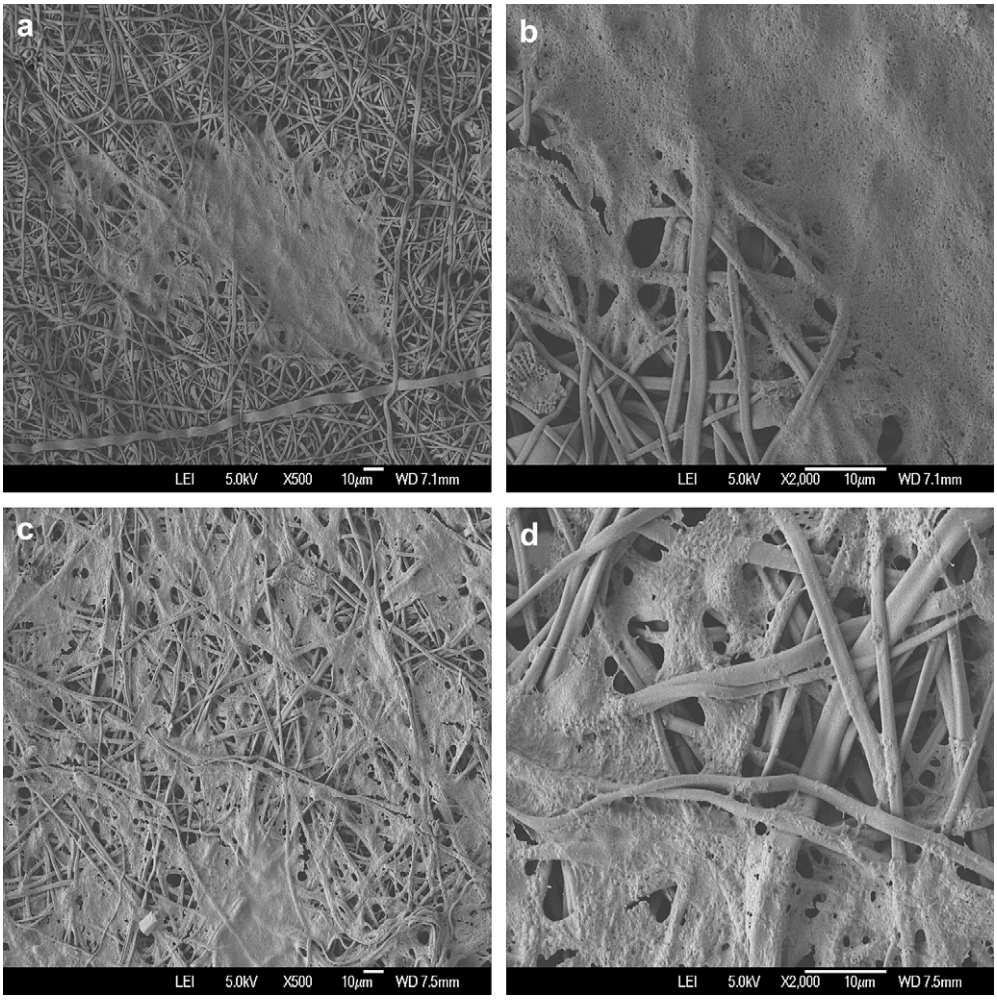

Fig. 8. SEM images obtained from the nonwoven mats after 10 days culture, preceded by cell fixation and dehydration procedure, for (a-b) PLLA and (c-d) **2**$_{74\text{-}26}$. Magnification: 500× (left side) or 2000× (hand side). Scale bar: 10 μm.

viewpoint, the surface energy can be considered as the sum of polar (or non-dispersive) and dispersive components [40,44]. The surface energy was calculated [44,45] by using advancing contact angle measurements in two different test liquids (water and diiodomethane) and Wu's harmonic mean method, in addition to the decomposition of the surface energy into the dispersive and polar components (Table 4). The surface energy obtained for PLLA agrees very well with those from literature: 39 mN m^{-1} [46], 42 mN m^{-1} [47], and 40 mN m^{-1} [48]. The values obtained for the samples of **2** are similar to each other and intermediate between those of PLLA and **3**. For comparison, Table 4 also shows the surface energy of collagen (48 mN m^{-1}) [49]. Collagen is an extracellular matrix protein that provides an attachment framework for adhesion and growth of specific cells *in vivo* and for cell attachment onto various substrates *in vitro* [49]. It is expected that the closer the product's surface energy with that of collagen, the higher will be the resulting cell adhesion.

3.5. Scaffold production through electrospinning

The unique ability of a scaffold to allow cell attachment and proliferation is dependent on its surface properties. Electrospinning provides a very special surface architecture, with multiple adhesion points and porous structure that has proven, in recent years, to be very efficient for cell culture and tissue engineering. In spite of several efforts to model its behavior in order to project its use, it still remains as a very empirical and often hard to control process. Nonetheless, boundary conditions were found to produce nanofibers from the chain extended copolymers.

Although all samples of **2** were successfully electrospun from their solutions in dichloromethane/*N*,*N*-dimetilformamide, **3** (as well as binary blends formed by PLLA and **2**$_{74\text{-}26}$) produced fibers mats containing a great amount of beads, an artifact known for systems of low average molar mass [24]. Fig. 4 displays the variation of fiber average diameter against the solution concentration for **2**$_{74\text{-}26}$. The fiber diameter increases with increasing polymer concentration in the solution (Fig. 4), consistent with the literature data [21,50]. Likewise, bead formation was also observed below a concentration threshold. The number of beads diminishes with the increase of the polymer concentration, also consistent with the literature data [24]. Since the concentration at 9% (w/v) presented low bead formation with fair fiber diameters, it was used as standard hereafter for the samples of **2**, whereas for PLLA the concentration used was 5% (w/v).

Fig. 5 shows the variation of fiber diameter against IS mass composition obtained for the samples of **2** by electrospinning. The fiber diameters obtained are similar, except that for **2**$_{64\text{-}36}$, which presented a higher value. Fig. 6 shows that electrospun fibers presenting a relatively low number of beads could be attained by using an intermediate concentration.

The diffraction patterns obtained by WAXD for the electrospun mats (previously dried at 40 °C for three days) from PLLA and **2** samples were acquired for comparison. All the samples displayed diffraction profiles characteristic of non-crystalline polymers (Supplementary Material 5), similar to the data reported in the literature for as-spun fibers [24]. These findings suggest that the electrospun mats used in the cell adhesion and proliferation studies (see below) were completely amorphous, despite the semi-crystalline nature of PLLA and **2** samples.

3.6. Fibroblast attachment and proliferation

Fibroblasts have become the prototypical cell for culture studies. They present high capacity for synthesis of several proteins and glycoproteins, making them highly adherent and resistant, hence easy to assay. The 3T3-L1 lineage is an embryonic adipose-like cell from Swiss albino mice with fibroblast morphology, widely used as a model cell for adherence, proliferation, gene expression, and differentiation studies. Here, 3T3-L1 cells were seeded onto electrospun mats made from solutions of the chain extended copolymers **2**. Care was taken in order to remove residual solvent from the samples. Since the objective was the evaluation of the effect of isosorbide succinate moiety inclusion into PLLA backbone, a similar electrospun mat made from PLLA homopolymer was used for comparison.

MTT assay was carried out to monitor 3T3-L1 cell growth. Since the assay washes out the non-adherent cells and it is specific to viable living cells, it reflects not only the ability of the scaffold for cell attachment and proliferation, but also its cytotoxicity. Proliferation was followed within a maximum period of 10 days. MTT results in Fig. 7 show that cell growth and proliferation for copolymers **2** were roughly twice higher in comparison to PLLA. In spite of the low rate of proliferation observed, the distinction is already apparent on day 3, clearly indicating the beneficial effect of IS blocks on the PLLA structure.

The significance of the data obtained at the end of 10 days growth period was evaluated by means of a two-way ANOVA test. The results show that the difference of the cell growth and proliferation of samples **2** compared to PLLA is statistically significant, regarding the significance level chosen (5%, 1%, or 0.1%; see Fig. 7). On the other hand, the data obtained for the different copolymers are not statistically different in relation to each other.

The 3T3-L1 proliferation was also analyzed by SEM imaging in order to infer on the cell adhesion and interaction with the 2-D scaffold structure. Fig. 8 shows the SEM images obtained for $\mathbf{2}_{74\text{-}26}$ and PLLA samples after 10 days of growth. The images clearly show that the samples from the copolymers present a greater cell density than that from PLLA. They also show that plateau phase of cell growth was not attained and the comparison of MTT study is, hence, valid. In addition, SEM images of Fig. 8 and of early stages (not shown) reveal that there are no significant morphological differences among cells as compared to those grown onto PLLA.

The findings can be associated with the greater surface energy observed for the scaffolds made from **2**, on account of the incorporation of IS into PLLA main backbone, and/or the better attachment sites afforded by the PIS blocks.

4. Conclusion

Block copolymers composed of LLA and IS with mass composition ratio in the range of 86/14 to 64/36% were successfully synthesized in two steps: (1) from bulk ring-opening copolymerization with L-lactide and PIS, in the presence of $SnOct_2$ as the reaction catalyst, giving rise to low molecular block copolymers, (2) followed by chain extension of the products via HDI and chloroform as chain extensor and solvent. PLLA homopolymer was also successfully obtained in bulk from ROP with L-lactide and $SnOct_2$. TG and DSC data showed that the copolymers and PLLA homopolymer presented similar thermal stabilities and glass transition temperatures. DSC and, especially, WAXD findings showed that the degree of crystallinity of the copolymers decreased as increased the incorporation of IS, which could be advantageous for faster biodegradation rate. The copolymers presented a higher surface energy (54 mN m^{-1}) than that of PLLA (40 mN m^{-1}). Nonwoven mats were successfully produced by electrospinning process from the copolymers and PLLA solutions, while the attempts to obtain electrospun fibers from the chain extended PIS solutions failed.

The study of fibroblast 3T3-L1 cells culture onto the electrospun nonwoven mats demonstrated that the block copolymers produce better scaffolds for fibroblast cell adhesion and proliferation than PLLA. MTT assays revealed a growth twice as fast for the copolymer as compared to PLLA homopolymer, a result confirmed by SEM. These findings must be related to the higher surface energy presented by the copolymers and/or the better anchorage sites provided by PIS blocks. This adds new potential in the uses of isosorbide-derived polyesters as biomaterials.

Acknowledgments

The authors wish to thank Capes, CNPq, and Fapesp for financial support.

Appendix. Supplementary data

Supplementary data associated with this article can be found in the online version, at doi:10.1016/j.polymer.2009.10.048.

References

[1] Garlotta D. J Polym Environ 2002;9:63–84.
[2] Kricheldorf HR. Chemosphere 2001;43:49–54.
[3] Middleton JC, Tipton AJ. Biomaterials 2000;21:2335–46.
[4] Tokiwa Y, Jarerat A. Biotechnol Lett 2004;26:771–7.
[5] Braun D, Bergmann M. J Prakt Chem 1992;334:298–310.
[6] Majdoub M, Loupy A, Flèche G. Eur Polym J 1994;30:1431–7.
[7] Okada M, Okada Y, Aoi K. J Polym Sci, Part A: Polym Chem 1995;33:2813–20.
[8] Casarano R, Petri DFS, Jaffe M, Catalani LH. J Braz Chem Soc 2009;20:1414–24.
[9] Kricheldorf HR, Behnken G, Sell M. J Macromol Sci, Part A: Pure Appl Chem 2007;44:679–84.
[10] Thiem J, Lüders H. Polym Bull 1984;11:365–9.
[11] Malhotra SV, Kumar V, East A, Jaffe M. The Bridge (NAE) 2007;37:17–25.
[12] Chatti S, Kricheldorf HR. J Macromol Sci, Part A: Pure Appl Chem 2006;43:967–75.
[13] Grijpma DW, Pennings AJ. Macromol Chem Phys 1994;195:1633–47.
[14] Pietrzak WS, Sarver D, Verstynen M. Bone 1996;19:109s–19s.
[15] Townsend KJ, Busse K, Kressler J, Scholz C. Biotechnol Prog 2005;21:959–64.
[16] Yoon J-S, Jung H-W, Kim M-N, Park E-S. J Appl Polym Sci 2000;77:1716–22.
[17] Wang Y-W, Yang F, Wu Q, Cheng Y-C, Yu PHF, Chen J, et al. Biomaterials 2005;26:755–61.
[18] Ma Z, Gao C, Gong Y, Shen J. Biomaterials 2003;24:3725–30.
[19] Ishaug-Riley SL, Okun LE, Prado G, Applegate MA, Ratcliffe A. Biomaterials 1999;20:2245–56.
[20] Shin YM, Hohman MM, Brenner MP, Rutledge GC. Polymer 2001;42:9955–67.
[21] Boland ED, Wnek GE, Simpson DG, Pawlowski KJ, Bowlin GL. J Macromol Sci, Part A: Pure Appl Chem 2001;A38:1231–43.
[22] Eichhorn SJ, Sampson WW. J R Soc Interface 2005;2:309–18.
[23] Mckee MG, Layman JM, Cashion MP, Long TE. Science 2006;311:353–5.
[24] Ramakrishna S, Fujihara K, Teo W-E, Lim T-C, Ma Z. An introduction to electrospinning and nanofibers. New Jersey: World Scientific; 2005.
[25] Piskin E, Bolgën N, Egri S, Isoglu IA. Nanomedicine 2007;2:441–57.
[26] Gogolewski S, Jovanovic M, Perren SM, Dillon JG, Hughes MK. Polymer Degrad Stab 1993;40:313–22.
[27] Adamson AW. Physical chemistry of surfaces. New York: John Wiley & Sons; 1990.
[28] Kowalski A, Duda A, Penczek S. Macromolecules 2000;33:7359–70.
[29] Ryner M, Stridsberg K, Albertsson A-C, von Schenck H, Svensson M. Macromolecules 2001;34:3877–81.

[30] Backus JK, Blue CD, Boyd PM, Cama FJ, Chapman JH, Eakin JL, et al. Polyurethanes. In: Kroschwitz JI, editor. Encyclopedia of polymer science and engineering, vol. 13. New York: John Wiley & Sons; 1985. pp. 243–303.
[31] Kylmae J, Seppaelae JV. Macromolecules 1997;30:2876–82.
[32] Hiki S, Miyamoto M, Kimura Y. Polymer 2000;41:7369–79.
[33] Adamus G, Rizzarelli P, Montaudo MS, Kowalczuk M, Montaudo G. Rapid Commun Mass Spectrom 2006;20:804–14.
[34] Bluhm TL, Hamer GK, Marchessault RH, Fyfe CA, Veregin RP. Macromolecules 1986;19:2871–6.
[35] Shyamroy S, Garnaik B, Sivaram S. J Polym Sci, Part A: Polym Chem 2005;43:2164–77.
[36] Wang Y, Funari SS, Mano JF. Macromol Chem Phys 2006;207:1262–71.
[37] Storbeck R, Rehahn M, Ballauff M. Makromol Chem 1993;194:53–64.
[38] Kricheldorf HR. J Macromol Sci, Rev Macromol Chem Phys 1997;C37:599–631.
[39] Thiem J, Lueders H. Makromol Chem 1986;187:2775–85.
[40] Garbassi F, Morra M, Occhiello E. Polymer surfaces: from physics to technology. New York: John Wiley & Sons; 1994. pp. 161–331.
[41] Vogler EA. Adv Colloid Interface Sci 1998;74:69–117.
[42] Janorkar AV, Metters AT, Hirt DE. Macromolecules 2004;37:9151–9.
[43] Inagaki N, Narushima K, Tsutsui Y, Ohyama Y. J Adhes Sci Technol 2002;16:1041–54.
[44] Bouali B, Ganachaud F, Chapel J-P, Pichot C, Lanteri P. J Colloid Interface Sci 1998;208:81–9.
[45] Yang J, Bei J, Wang S. Biomaterials 2002;23:2607–14.
[46] Smith R, Pitrola R. J Appl Polym Sci 2002;83:997–1008.
[47] Yang J, Wan Y, Tu C, Cai Q, Bei J, Wang S. Polym Int 2003;52:1892–9.
[48] Ji Y, Li X-T, Chen G- Q. Biomaterials 2008;29:3807–14.
[49] Harnett EM, Alderman J, Wood T. Colloids Surf, B 2007;55:90–7.
[50] Pham QP, Sharma U, Mikos AG. Tissue Eng 2006;12:1197–211.